Received: 3 April 2024 | Revised: 2 May 2024 | Accepted: 20 May 2024

DOI: 10.1002/fft2.435

FOOD FRONTIERS Open Access

RESEARCH ARTICLE

The orchestrated feature of *Cornus kousa* fruit and gut microbiota against obesity via integrated pharmacology

Ki-Kwang Oh | **Sang-Jun Yoon** | **Sang Youn Lee** | **Satya Priya Sharma** | **Sung-Min Won** | **Jin-Ju Jeong** | **Dong Joon Kim** | **Ki-Tae Suk**

Institute for Liver and Digestive Diseases, College of Medicine, Hallym University, Chuncheon, South Korea

Correspondence
Ki-Tae Suk, Institute for Liver and Digestive Diseases, College of Medicine, Hallym University, Chuncheon 24252, South Korea.
Email: ktsuk@hallym.ac.kr

Funding information
The Basic Science Research Program through the National Research Foundation of Korea (NRF) funded by the Ministry of Education, Science and Technology, Grant/Award Numbers: NRF2019R1I1A3A01060447, NRF-2020R1A6A1A03043026; Bio Industrial Technology Development Program funded by the Ministry of Trade, Industry and Energy (MOTIE, Korea), Grant/Award Number: 20018494; Hallym University Research Fund; Korea Institute for Advancement of Technology funded by the Ministry of Trade, Industry and Energy (MOTIE, Korea), Grant/Award Number: P0020622

Abstract

Cornus kousa fruit (CKF) has been utilized as anti-obesity supplementation in East Asia, including Korea, and gut microbiota (GM) might have synergistic effects on obesity (OB) via its interplay. We aimed to decode molecule(s), mechanism(s), and target(s) on interplay between CKF and GM via network pharmacology analysis. The final targets were analyzed by protein–protein interaction (PPI) networks and a bubble plot. The GM interacted with significant targets identified by the gutMGene database. The relationships among CKF or GM, signaling pathways, targets, and molecules (CGSTM) were plotted by R package. Finally, molecular docking assay and density functional theory (DFT) were performed to validate its affinity. The final targets (22) were selected on OB-responded targets, indicating that interleukin-6 (IL6) was the most crucial protein-coding target on PPI networks. A bubble plot and CGSTM networks suggested that the advanced glycation end-receptor for advanced glycation end products signaling pathway in diabetic complications is inhibited by CKF and peroxisome proliferator–activated receptor (PPAR) signaling pathway is activated by GM. As the most stable conformers, IL6-equol complex was attributed to GM, and PPAR alpha-linoleic acid, PPAR delta-stearic acid, and fatty acid–binding protein 4-dimethyl 2,3-bis(1,3-dimethylindol-2-yl) fumarate complex were attributed to CKF. Noticeably, stearic acid was removed by DFT analysis; all other three molecules were proposed as good electron donators with the higher electronegativity compared with a standard drug (Orlistat). This study shows that integrated pharmacological analysis can enable to decode the unknown relationships between CKF and GM. Overall, this study reveals that the combination of CKF and favorable GM might exert dual therapeutic effects on OB.

KEYWORDS
AGE-RAGE signaling pathway in diabetic complications, *Cornus kousa* fruit, gut microbiota, PPAR signaling pathway

This is an open access article under the terms of the Creative Commons Attribution-NonCommercial-NoDerivs License, which permits use and distribution in any medium, provided the original work is properly cited, the use is non-commercial and no modifications or adaptations are made.
© 2024 The Author(s). *Food Frontiers* published by Nanchang University, Northwest University, Jiangsu University, Fujian Agriculture and Forestry University, International Association of Dietetic Nutrition and Safety and John Wiley & Sons Australia, Ltd.

1 | INTRODUCTION

Obesity (OB) influences negatively diverse metabolic disorders, such as cardiovascular diseases, diabetes, hypertension, and heart failure, which account for around one fifth of cancer types (Artham et al., 2009; Preuss et al., 2010). In 2014, more than 2 billion people, approximately one third of the world population, were overweight, or around 5% of mortality is liable to OB (Tremmel et al., 2017). OB is represented by excessive accumulation of fat in the tissue, leading to unbalanced energy, inappropriate secretion of appetite hormones, and insulin resistance (Oh, 2022). Body mass index is a criterion to assess OB; its clinical standard is more than 30.0 or higher (Nuttall, 2015). The most significant therapeutics for anti-obesity (AOB) is to block the absorption of lipid in the body tissue and, furthermore, to dampen the decomposition and transportation of fat via metabolic pathways (Fan et al., 2021). Up to now, five representative medications (Orlistat, Phentermine/topiramate, Naltrexon/bupropion, Liraglutide, and Lorcaserin) against OB have been taken to alleviate its pathophysiological mechanism in spite of some side effects (insomnia, anxiety, depression, diarrhea, and vomiting) (Tak & Lee, 2021). At present, a therapeutic strategy to diminish the adverse effects might be optimally selective for the obese. For the past decade, natural products have been an increasingly significant therapeutic resource for the alleviation in OB due to its low negative side effects (Chandrasekaran et al., 2012). In recent years, the ethanolic fraction of *Cornus kousa* leaves has exerted potent AOB efficacy by downregulating adipogenesis and lipogenesis in 3T3-L1 cells (Khan et al., 2018). Commonly, leaves and fruits possess the majority of chemical constituents; however, fruits comprised more notable chemical compounds and contained higher chemo-diversity (Schneider et al., 2021). Thus, we aimed to elucidate the therapeutic value on *C. kousa* fruit (CKF) in the treatment of OB. The AOB effects of herbal organic compounds are mediated by synchronizing lipolysis and lipogenesis (Rayalam et al., 2008). However, during the past decades, the bona fide efficacy of natural products has been controversial, although noticeable progress has been made in treating OB on herbal remedies (Liu et al., 2017). Additionally, the exact pharmacological mechanisms of natural products against OB have yet to be determined.

From another viewpoint, the gut microbiota (GM) plays an important role in alleviating OB, and therefore, commensal bacteria modulate numerous genes to improve the response of the immune system (Cheng, Zhang, et al., 2022; Zheng, Liwinski, et al., 2020). Most recently, the diversity of the GM was found to have therapeutic effects in humans and in animal models of OB (Zheng, Chen, et al., 2022). A report demonstrated that the GM-derived metabolites (amino acids, lipid-like compounds, and bile acid derivatives, or byproducts of carnitine, choline, polyphenols, and purines) are involved in metabolic disorders of OB, along with insulin resistance, hyperglycemia, and dyslipidemia (Ejtahed et al., 2020). According to the study done to date, metabolites from GM could be useful agents in ameliorating OB.

In summary, we integrated the chemical constituents of CKF and metabolites of GM to investigate the combination efficacy in the treatment of OB. With a bird's-eye view, we postulated that the integrative application of natural compounds from CKF and metabolites from the GM can alleviate OB.

It is imperative to utilize the network pharmacology (NP) concept to elucidate its combinatorial effects concerning OB. NP can unravel the biological mechanisms(s) of key effectors with extensive concept, which is defined as the paradigm shift from "one target, one ligand, one disease" to "network-integrated-multi component therapeutics" (Szumilak et al., 2021; Vetrivel et al., 2021). Additionally, the progressive development of bioinformatics, system biology, and cheminformatics is an emerging trend to discover new agents or repurpose existing drugs (Loging et al., 2011). Furthermore, NP methodology might be a powerful tool to decode promising new drugs to dampen metabolic disorders, including AOB (Li et al., 2017). From this perspective, we devised a new methodology to reveal AOB effects via a combination of agents from CKF and GM. First, chemical constituents from CKF were detected by Agilent 7890A gas chromatography–mass spectrometry (GC–MS) and the drug-likeness properties were evaluated by Lipinski's rule. The targets related to the compounds were retrieved by the Similarity Ensemble Approach (SEA) and SwissTargetPrediction (STP), and common targets were identified by a Venn diagram. Second, OB-responding targets were sorted by public bioinformatics, and the final targets were selected. The final overlapping targets were used as elements to analyze protein–protein interaction (PPI) networks and generate a bubble plot. Third, we utilized the GM database (gutMGene) to construct relationships in CKF and GM, including signaling pathways, targets, and molecules (CGSTM). Then, we performed a molecular docking assay (MDA) to verify the effects of the compound(s) on target(s) in key signaling pathway(s). Finally, density functional theory (DFT) was conducted to evaluate the chemical stability and reactivity of the key targets. The workflow of this study is depicted in Figure 1.

2 | MATERIALS AND METHODS

2.1 | The collection and extraction of CKF

CKF was collected from (latitude: 37.52, longitude: 128.29) Gangwon-do, Korea, in October 2022. The CKF (Vouch number: A237) was dried in a shaded room with an air ventilator maintaining 20–22°C for 3 weeks, and its seeds were removed from the dried CKF. The CKF removed seeds pulverized with a blender. Around 30 g of CKF powder was extracted with 500 mL ethyl alcohol (Samchun) for 2 weeks and repeated three times to obtain higher yield rate. The ethyl alcohol extract was collected, used on Whatman filter paper No. 1 (Whatman, Model no. WF1-1850), and evaporated with a vacuum evaporator (IKA-RV8) at 40°C. The extraction amount after evaporating was 7.78 g (yield rate: 25.9%), which was calculated as

$$\text{Yield rate (\%)} = (\text{Evaporated extraction weight}/\text{Dried CKF weight}) \times 100$$

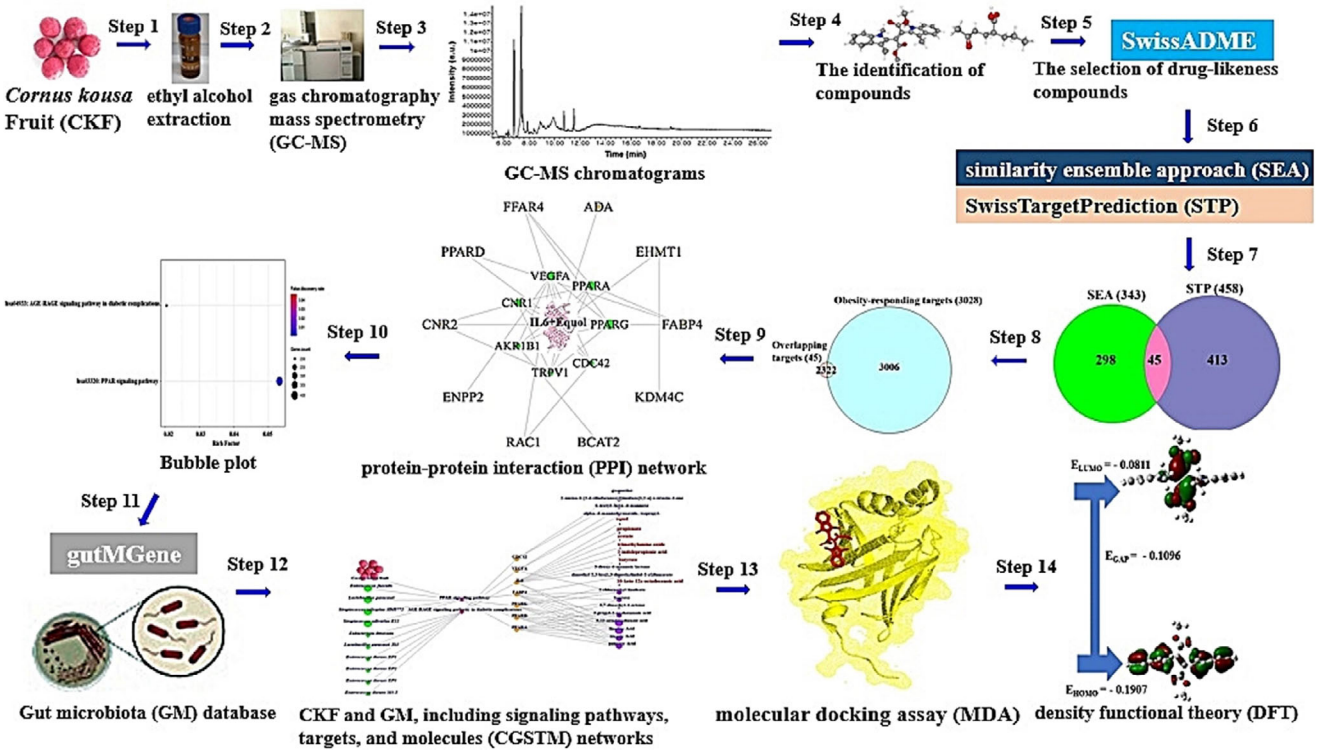


FIGURE 1 The workflow of this study. CGSTM, CKF and GM, including signaling pathways, targets, and molecules; CKF, *Cornus kousa* fruit; DFT, density functional theory; E_{GAP}, energy gap; E_{HOMO}, energy of the highest occupied molecular orbital; E_{LUMO}, energy of the lowest unoccupied molecular orbital; GC–MS, gas chromatography-mass spectrometry; GM, gut microbiota; MDA, molecular docking assay; SEA, similarity ensemble approach; STP, SwissTargetPrediction.

2.2 | The GC–MS analysis condition

We employed Agilent 7890A (Agilent) to conduct GC–MS, its column was selected as DB-5 (30 m × 0.25 mm × 0.25 μm) (Agilent) with reverse phase. The GC–MS was kept at 100°C for 2.1 min, rising gradually to 300°C at a rate of 25°C/min and was maintained for 20 min. Injection port temperature was 250°C, helium flow rate was 1.5 mL/min, and the ionization voltage was 70 eV. The split mode of sample injection was at 10:1, and the MS detection range consisted of 35–900 (*m/z*). The fragmentation modes of MS were compared with the W8N05ST Library MS database (analyzed January 13, 2023).

2.3 | The utilization of the web-accessible public databases

The rapid development of public databases' technologies, including bioinformatics and cheminformatics, provides a great amount of data produced that is in gradual improvement in diverse research fields. Utilizing the significant bio databases in drug discovery or development is a powerful analytical technology. Specifically, we merged the important databases to cull the valuable components in intricated microbiome research. We categorized the accessible database repositories in Table 1.

2.4 | Identification of chemical compounds in CKF and filtering of drug-resemblance biomolecules

The chemical compounds in CKF were identified by GC–MS analysis, converting into Simplified Molecular Input Line Entry System (SMILES) format via PubChem (https://pubchem.ncbi.nlm.nih.gov/) (accessed on February 19, 2023). Then, we employed Lipinski's rule to screen drug-resemblance biomolecules (DRBs) through SwissADME (http://www.swissadme.ch/) (accessed on February 19, 2023). As a criterion of cell permeability, we adopted topological polar surface area (TPSA) value with less than 140 Å^2 (a threshold) (Matsson & Kihlberg, 2017).

2.5 | Targets associated with DRBs from CKF or OB

The targets related to DRBs were browsed by SEA (Keiser et al., 2007) and STP (Daina et al., 2019) on "Homo Sapiens" mode. The relationship between targets and DRBs was constructed by utilizing the two databases, which confirmed its effectiveness through experimentation: Approximately 80% of drug candidates line up with SEA database, and additionally, the significant targets on Cudraflavone C were sorted by STP, and its bioactivities were confirmed by experiment (Singh et al.,

TABLE 1 The profiles of available databases for the study.

No.	Databases	Specification	URL
1	AutoDock 1.5.6	A program for virtual screening of molecules to targets	https://mybiosoftware.com/autodock-4-2-3-autodocktools-1-5-6-suite-automated-docking-tools.html
2	DisGeNET	The collective repository related to human diseases	https://www.disgenet.org/
3	Gaussian 16 W	Computational chemistry software for DFT	no available: commercial item
4	GaussView 6.0	Chemical interface program	https://gaussview.software.informer.com/6.0/
5	gutMGene	The database of gut microbiota and its metabolites	http://bio-annotation.cn/gutmgene
6	LigPlot++	A program to generate 2D ligand-protein interaction diagrams	https://www.ebi.ac.uk/thornton-srv/software/LigPlus/download.html
7	Online Mendelian Inheritance in Man (OMIM)	Human disease database associated with targets	https://www.omim.org/
8	PubChem	A database of chemical information	https://pubchem.ncbi.nlm.nih.gov/
9	RCSB PDB	The protein-structure based database	https://www.rcsb.org/
10	R package	A software for networking visualization	https://www.r-project.org/
11	Similarity Ensemble Approach (SEA)	A database to identify targets on compounds	https://sea.bkslab.org/
12	STRING	A database for protein-protein interaction (PPI) networks	https://string-db.org/
13	SwissADME	A database to confirm the drug-like properties	http://www.swissadme.ch/
14	SwissTargetPrediction (STP)	A database to estimate the targets on biomolecules	http://www.swisstargetprediction.ch/
15	Venn Diagram Plotter	Venn diagram proportional drawing tool	http://www.softsea.com/review/Venn-Diagram-Plotter.html

Abbreviation: DFT, density functional theory.

2021; Soo et al., 2017). The targets related to DRBs were identified by DisGeNET (https://www.disgenet.org/) (accessed on February 20, 2023) and OMIM (https://www.omim.org/) (accessed on February 20, 2023). The final intersecting targets between sorted DRB-associated targets and OB-responding targets were established and visualized via a Venn diagram plotter.

2.6 | The protein–protein interaction (PPI) networks and a bubble chart

The PPI networks were constructed to discern what the most significant target is among intersecting targets. We adopted STRING (https://string-db.org/) (accessed on February 21, 2023) database for the PPI construction, and a bubble chart was plotted by R package. The bubble chart was built by a rich factor defined as the number of differentially expressing targets annotated in each pathway (Zhang et al., 2019). Based on the bubble chart, we could identify an activating signaling pathway and an inhibitive signaling pathway. Hence, we considered key mechanisms in the treatment of OB.

2.7 | CKF and GM, including signaling pathways, targets, and molecules (CGSTM) networks

We employed gutMGene database to incorporate the metabolites of GM; thereby, assembled networks were defined as CGSTM networks. The CGSTM networks were constructed as a map based on degree of value (DV). In the incorporated networks, taking CKF or GM, signaling pathways, targets, and metabolites as nodes, its relationships were indicated as edges. The green circles represented GM, red circles stood for signaling pathways, orange circles indicated targets, and purple circles described metabolites. Then, the gray line indicated its relationships, and the metabolites from GM represented with red text. The integrated CGSTM networks were plotted by R Package.

2.8 | The verification for molecular docking assay (MDA)

We performed the MDA to select the uppermost biomolecule(s) from two key signaling pathways. Based on MDA, we can identify what

the most significant metabolite(s) are stemmed from either GM or CKF. The targets were retrieved by RCSB PDB (https://www.rcsb.org/) (accessed on February 22, 2023). The extracted .pdb format was transformed into .pdbqt format via Autodock tool (https://autodock.scripps.edu/) (accessed on July 22, 2023) to perform the MDA. Then, the DRBs related to the targets were determined .sdf format by PubChem, and the.sdf configuration was altered into.pdb file via Pymol.

2.9 | MDA of biomolecules on targets related to key signaling pathways

The MDA was analyzed to elucidate its affinity of the biomolecules and targets linked to two key signaling pathways to be functioned as effector(s). The center of targets on the two key signaling pathways was $x = 11.213$, $y = 33.474$, $z = 11.162$, and $x = 8.006$, $y = -0.459$, $z = 23.392$, respectively. The cubic box size of active site was $x = 40$ Å, $y = 40$ Å, $z = 40$ Å. LigPlot+ 2.2 was utilized to describe the interaction of 2D binding on hydrophobic and hydrophilic bonds (https://www.ebi.ac.uk/thornton-srv/software/LigPlus/) (accessed on February 23, 2023) (Laskowski & Swindells, 2011).

2.10 | The reactivity of key biomolecules via frontier molecular orbitals (FMOs)

Based on the Lee–Yang–Parr correlation functional theory at the 6-31G++ (d,p), the key biomolecules, including a positive control, were completely formatted utilizing GaussView 6.0 and Gaussian 16 W software. The Gaussian16 program package was set up as follows:

(i) Gaussian Calculation Setup: Job Type; optimization.
(ii) Method: DFT; B3LYP; Basis set: 6-31G.
(iii) Link 0: Memory Limit; 1500 MB, Shared Processors; 4.
(iv) MO Editor: Visualize; Add Type: HOMO, LUMO.

This setup methodology was to obtain molecular orbitals (MOs): lowest occupied MO (LUMO) and highest occupied MO (HOMO). To assess the reactivity of key molecules, energy gap (eV), hardness (η), softness (S), and electronegativity (χ) were calculated by the following formulae (Adole, 2021):

$$\text{Energygap} = \text{HOMO} - \text{LUMO}$$

$$\eta = (\text{LUMO} - \text{HOMO})/2$$

$$S = 1/\eta$$

$$\chi = -(\text{LUMO} - \text{HOMO})/2$$

3 | RESULTS

3.1 | Profiling of biomolecules from CKF

A total of 31 biomolecules from CKF (Figure 2a) were recorded by GC–MS (Figure 2b), which listed the biomolecule name, PubChem ID, retention time, area, and chemical taxonomy (Table S1). The 31 biomolecules were accepted by Lipinski's rule (molecular weight ≤500 g/mol; Moriguchi octanol–water partition coefficient ≤4.15; number of nitrogen or oxygen ≤10; number of NH or OH ≤5). The TPSA values as the cell permeability standard are less than 140 $Å^2$, and the chemical constituents confirmed by the filtering were considered DRBs (Table S2).

3.2 | Recognition of intersecting targets between SEA and STP databases

The targets associated with DRBs were identified by SEA and STP databases, indicating that targets were identified by SEA (343), STP (458), and each other (Table S3). The Venn diagram plotter represented the intersecting targets (45) as important targets linked to DRBs (Table S3) (Figure 2c).

3.3 | Identification of the final overlapping targets between OB-responding targets and the intersecting targets (45)

The number of 3028 targets connected to occurrence and progression of OB was browsed by DisGeNET and OMIM databases (Table S3) (Figure 2d). Additionally, the Venn diagram plot showed that 22 targets were protein-coding genes overlapping between CKF-related targets and OB-responding targets. However, 4 of the 22 targets (PDCD4, ADH1B, GSTK1, and OXER1) were not correlated with one another.

3.4 | PPI networks and key signaling pathways via a bubble plot

The PPI networks were constructed by the R Package through STRING database, and the results suggested that interleukin-6 (IL6) had the greatest DV (12) among the 18 targets (18 nodes and 37 edges) (Table S4) (Figure 2e). A bubble plot showed that the peroxisome proliferator–activated receptor (PPAR) signaling pathway as an agonist and the advanced glycation end-receptor for advanced glycation end products (AGE-RAGE) signaling pathway in diabetic complications as an antagonist might exert therapeutic effect in OB (Table 2) (Figure 2f).

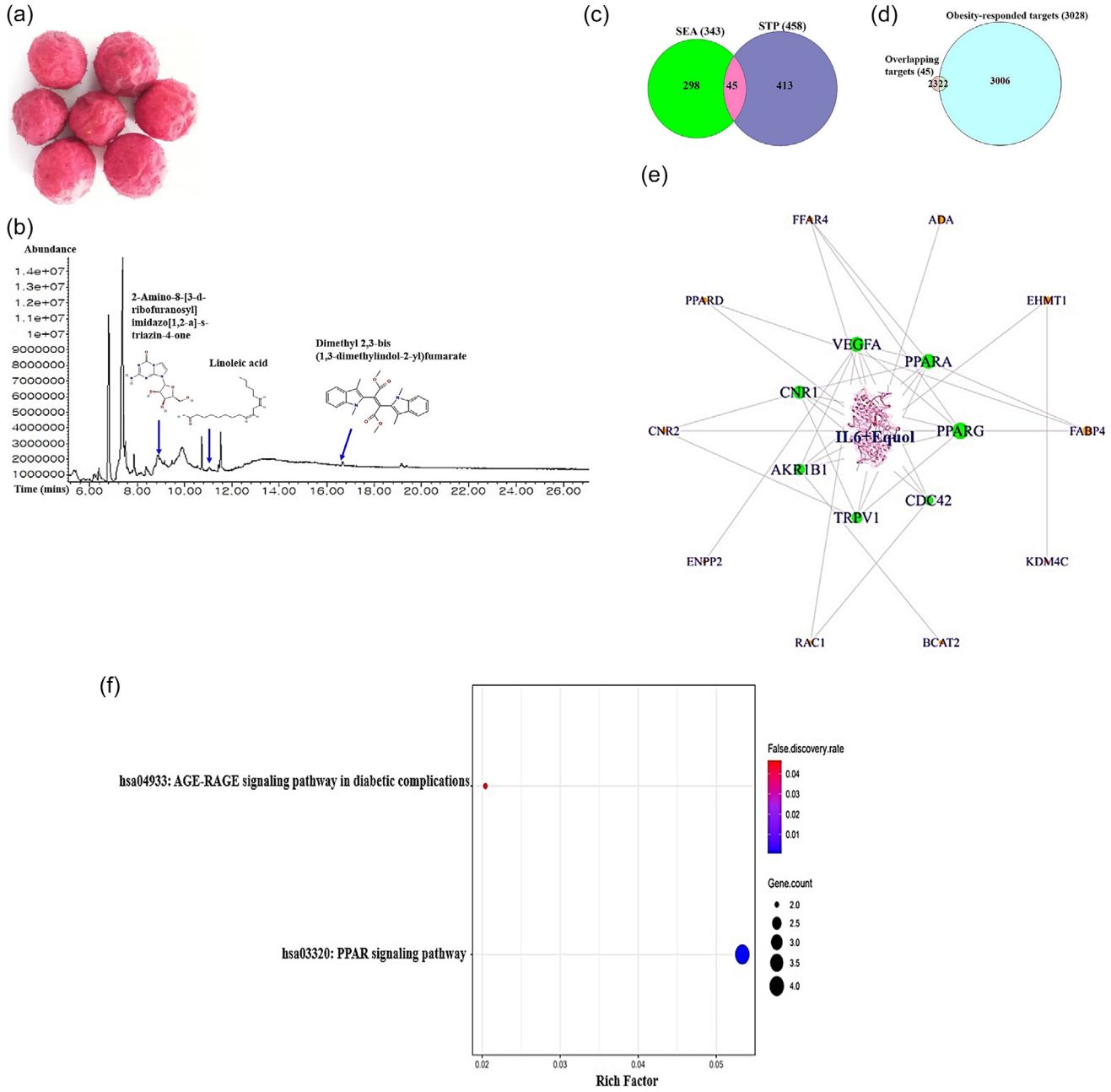


FIGURE 2 (a) The picture of *Cornus kousa* fruit (CKF); (b) GC–MS chromatography of CKF; (c) the number of 45 targets between Similarity Ensemble Approach (SEA) (343) and SwissTargetPrediction (STP) (458); (d) the number of 22 final targets between 45 targets and obesity (OB)-responding targets (3028); (e) the protein–protein interaction (PPI) networks (18 nodes and 37 edges); (f) a bubble plot of occurrence and development on OB.

TABLE 2 The targets of key signaling pathways on obesity (OB).

KEGG ID & Description	Target	False discovery rate
hsa03320: PPAR signaling pathway	PPARA, PPARD, PPARG, FABP4	0.00057
hsa04933: AGE-RAGE signaling pathway in diabetic complications	IL6, VEGFA, CDC42	0.0321

Abbreviations: AGE-RAGE, advanced glycation end-receptor for advanced glycation end products; CDC42, cell division cycle 42; FABP4, fatty acid–binding protein 4; IL6, interleukin 6; KEGG, Kyoto Encyclopedia of Genes and Genomes; PPARA, peroxisome proliferator–activated receptor alpha; PPARD, peroxisome proliferator–activated receptor delta; PPARG, peroxisome proliferator–activated receptor gamma; VEGFA, vascular endothelial growth factor-A.

3.5 | The CGSTM analysis with GM and CKF

The CGSTM networks include CKF, 10 GMs, 2 signaling pathways, 7 targets, and 21 metabolites, representing 41 nodes, and 59 edges. The CKF, *Enterococcus faecalis*, *Lactobacillus paracasei*, *Strepotococcus salivarius JIM8772*, and *S. salivarius K12* are related to PPAR signaling pathway on fatty acid–binding protein 4 (FABP4), PPAR alpha (PPARA), PPAR delta (PPARD), and PPAR gamma (PPARG) with 10 metabolites. *Eubacterium limosum*, *L. paracasei JS1*, *Enterococcus durans EP1*, *E. durans EP2*, *E. durans EP3*, *and E. durans M4-5* are associated with AGE-RAGE signaling pathway in diabetic complications on cell division cycle 42 (CDC42), vascular endothelial growth factor-A (VEGFA), and IL6 with 11 metabolites (Figure 3a). Hence, GM's metabolites and CKF biomolecules show that they have strong relationships that exert the therapeutic effects in treating OB.

3.6 | Molecular docking assay (MDA)

In the PPAR signaling pathway, MDA revealed that both linoleic acid and stearic acid with PPARA (PDB ID: 3SP6) and PPARD (PDB ID: 5U3Q) had valid docking scores of −6.0 and −6.8 kcal/mol, respectively (Figure 3b). For VEGFA (PDB ID: 3P9W) and PPARG (PDB ID: 3E00), there were no potent metabolites from CKF and GM. Noticeably, dimethyl 2,3-bis(1,3-dimethylindol-2-yl) fumarate had the most stable binding score (−6.7 kcal/mol) with FABP4 (PDB ID: 3P6D) (Figure 3c). The potential ligands that interacted with the PPAR signaling pathway originated from CKF. In the AGE-RAGE signaling pathway in diabetic complications, IL6 (PDB ID: 4NI9) was associated with the following nine metabolites in DRBs from CKF and GM: (1) equol (PubChem ID: 91469), (2) 3-indolepropionic acid (PubChem ID: 3744), (3) 3-deoxy-d-mannoic lactone (PubChem ID: 541561), (4) linoleic acid (PubChem ID: 5280450), (5) 9,12-octadecadienoic acid (PubChem ID: 3931), (6) butyrate (PubChem ID: 104775), (7) acetate (PubChem ID: 175), (8) trimethylamine oxide (PubChem ID: 1145), and (9) propionate (PubChem ID: 104745). Among the nine metabolites, the most stable conformer was equol converted from *L. paracasei JS1*, which was −7.2 kcal/mol with valid binding energy (Figure 3d). Commonly, the active value of binding energy is less than −6.0 kcal/mol on AutoDock Vina (Shityakov & Förster, 2014). Next, for CDC42 (PDB ID: 3GCG), (1) 2-amino-8-[3-d-ribofuranosyl] imidazo[1,2-a]-s-triazin-4-one (PubChem ID: 15954620) produced by CKF formed the most stable complex with a binding energy of −6.8 kcal/mol (Figure 3e), followed by (2) guanosine (PubChem ID: 135398635). The significant metabolites in the AGE-RAGE signaling pathway in diabetic complications originated from CKF and GM. The detailed information of MDA is represented in Table S5.

3.7 | DFT verification of key molecules and a positive control

DFT was adopted to identify chemical reactivity (energy gap [eV], hardness [η], softness [S], and electronegativity [χ]) factors between key molecules and a positive control. Commonly, an acceptor or a donator can be identified based on the LUMO and HOMO levels. It has been suggested that equol, dimethyl 2,3-bis(1,3-dimethylindol-2-yl) fumarate, and 2-amino-8-[3-D-ribofuranosyl]imidazo[1,2-a]-*S*-triazin-4-one) had noticeable softness values (10.025, 18.248, and 9.706 eV), which were more stable than a standard medicine (Orlistat). Molecule stability is determined by the HOMO–LUMO energy gap, and the molecule with lower energy gap is linked to its softer property; the compound(s) with the characters can be considered the most significant agent(s) (Miar et al., 2021). Specifically, stearic acid with positive values on both LUMO and HOMO was removed because a positive HOMO would suggest that the physicochemical property can be ionized easily (De Lile et al., 2020). The detailed representation is depicted in Table 3 (Figure 3f).

4 | DISCUSSION

The CKF is known as herbal source to ameliorate OB; nevertheless, its effectors are yet to be reported completely, including its promising targets and mechanism(s). In this study, we employed GC–MS analysis to select the DRBs to be permeable in the cells.

In parallel, our aim was to establish the merged representation with biomolecules from CKF and GM, which will provide a new insight to clarify the specific relationships between the phytochemicals and GM. Up to date, the perspective viewpoints to demonstrate scientific pieces of evidence have been developed with data repository (Bresser et al., 2022). Thereby, we analyzed the interplay between CKF and GM in the treatment on OB with the assistance of rigorous bioinformatics: SEA (Keiser et al., 2007), STP (Gfeller et al., 2013), STRING (Szklarczyk et al., 2021), and gutMGene (Cheng, Qi, et al., 2022). Moreover, based on the quantum chemical analysis, we adopted DFT theory to confirm the chemical reactivity of key molecules. The reactivity was determined by energy gap, hardness, softness, and electronegativity through LUMO and HOMO values. The stability and reactivity of molecules may be attributed to E_{GAP}, which is a significant description to explain, such as hardness, softness, and electronegativity (Lucido et al., 2016; Pearson, 1986; Shahinozzaman et al., 2018; Silvarajoo et al., 2020). The greater the electronegativity, the more greatly that atom attracts the shared electrons, which is an index to measure the charge transfer in a molecule (Tantardini & Oganov, 2021). DFT was employed to establish a more accurate theory, suggesting that the three molecules had more stability, softness, and reactivity than a standard drug (Orlistat).

In this study, we have shown the combinatorial efficacy to relieve OB on PPAR signaling pathways and AGE-RAGE signaling pathways in diabetic complications. For example, a dietary mixture with 1% (weight/weight) linoleic acid for 4 weeks reduced body weight (BW) and white adipose tissue (WAT) density in mice experiment (Poirier et al., 2005). Likewise, a 1% and 1.5% (weight/weight) composition of linoleic acid for 21–28 days diminished BW and WAT amounts in obese mice (Wendel et al., 2008). It elicits that optimal treatment of linoleic acid might be an ameliorator for AOB. As an indole derivative, the pharmacological activity of dimethyl 2,3-bis(1,3-dimethylindol-2-yl) fumarate is yet to be confirmed. Our study suggests that dimethyl 2,3-

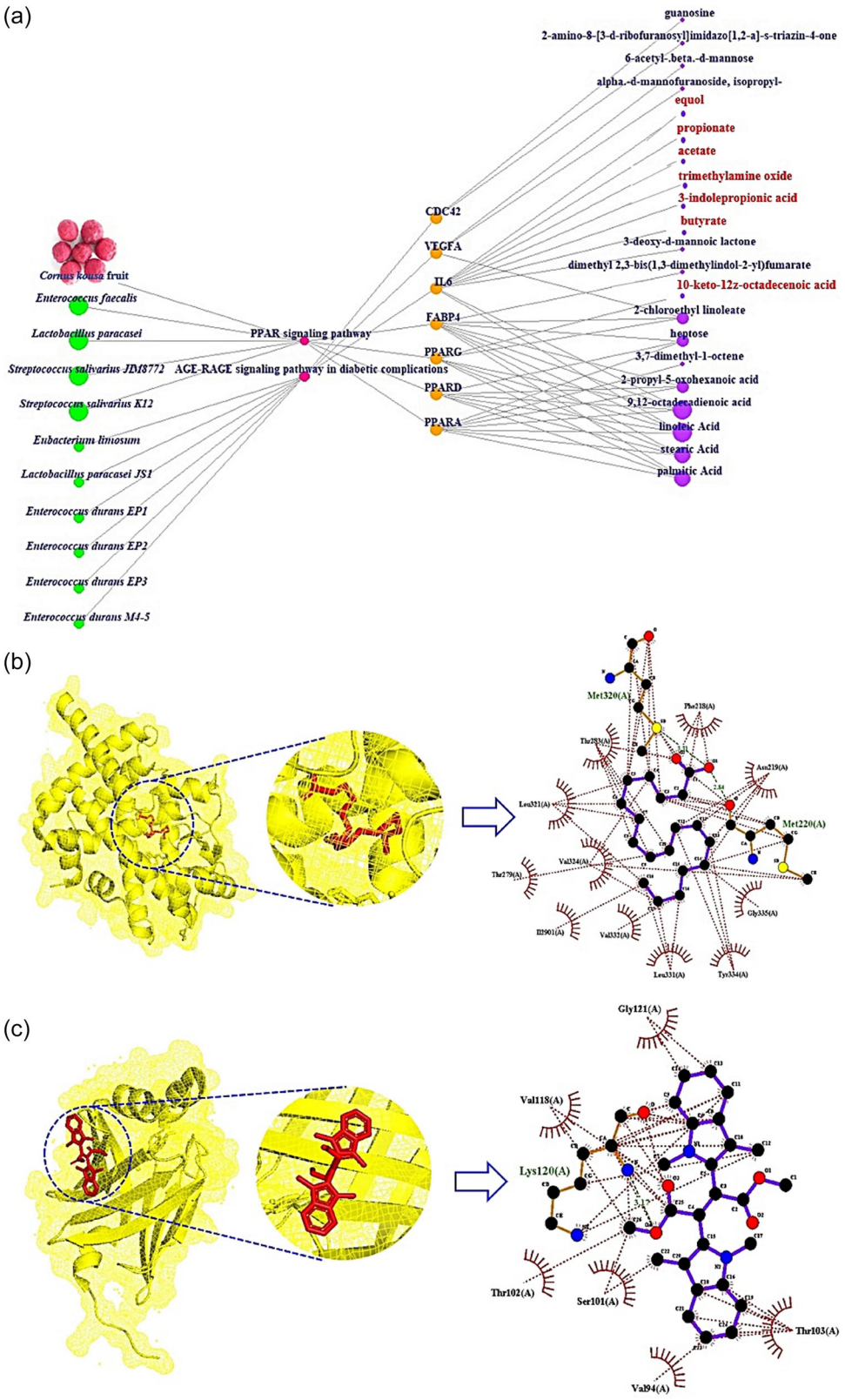


FIGURE 3 (a) *Cornus kousa* fruit (CKF) and gut microbiota (GM), including signaling pathways, targets, and molecules (CGSTM) networks (42 nodes and 59 edges). Red text: metabolites from GM. PPAR: peroxisome proliferator–activated receptor; AGE-RAGE: advanced glycation end-receptor for advanced glycation end products; CDC42: cell division cycle 42; VEGFA: vascular endothelial growth factor-A; IL6: interleukin-6; FABP4: fatty acid–binding protein 4; PPARG: PPAR gamma; PPARD: PPAR delta; PPARA: PPAR alpha. (b) PPARA-linoleic acid conformer. (c) FABP4-dimethyl 2,3-bis(1,3-dimethylindol-2-yl) fumarate conformer. (d) IL6-Equol conformer. (e) CDC42-2-amino-8-[3-D ribofuranosyl]imidazo[1,2-a]-*s*-triazin-4-one conformer. (f) Molecular orbital energy description and their energy gap of key molecules from CKF, GM and a standard drug (Orlistat). Green color orbitals: electrophilic groups; red color orbitals: nucleophilic groups.

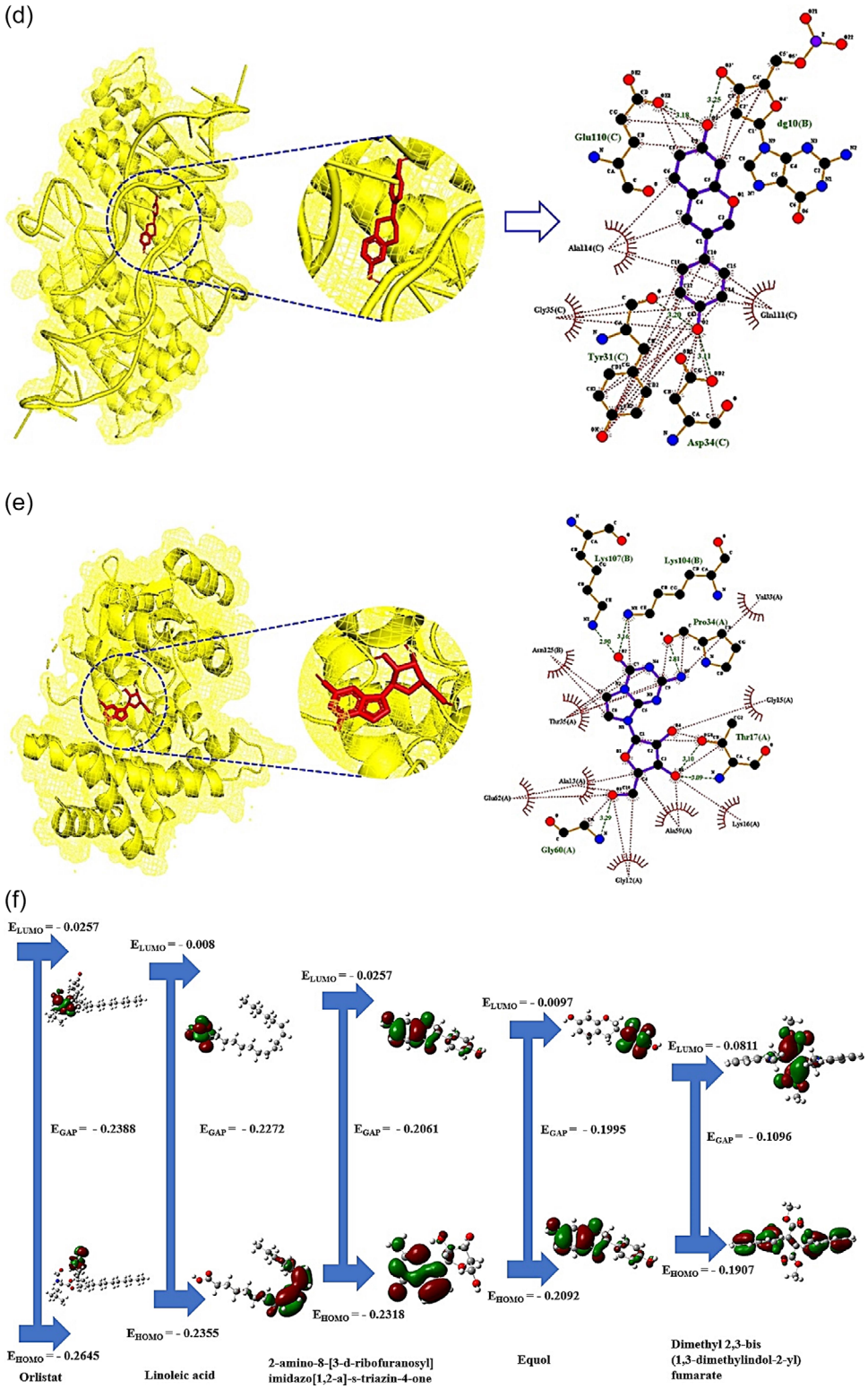


FIGURE 3 Continued

bis(1,3-dimethylindol-2-yl) fumarate might exert therapeutic effect on FABP4. As aforementioned above, linoleic acid and dimethyl 2,3-bis(1,3-dimethylindol-2-yl) fumarate are effectors to activate PPAR signaling pathway due to the highest rich factor on a bubble plot. Accordingly, the biomolecules from CKF were associated with activation on PPAR signaling pathway.

Next, in AGE-RAGE signaling pathway in diabetic complications, equol from GM is the most stable ligand on IL6, considering that equol

TABLE 3 The parameters of quantum kinetics of key compounds and a standard drug.

Molecules	LUMO	HOMO	E_{GAP} (eV)	η (eV)	S (eV)	χ (eV)
Orlistat*	−0.0257	−0.2645	−0.2388	0.1194	8.3766	−0.1194
Linoleic acid	−0.0082	−0.2355	−0.2272	0.1136	8.8017	−0.1136
2-amino-8-[3-D-ribofuranosyl]imidazo[1,2-a]-*S*-triazin-4-one	−0.0257	−0.2318	−0.2061	0.1030	9.7059	−0.1030
Equol	−0.0097	−0.2092	−0.1995	0.0998	10.0246	−0.0998
Dimethyl 2,3-bis(1,3-dimethylindol-2-yl)fumarate	−0.0811	−0.1907	−0.1096	0.0548	18.2482	−0.0548

Abbreviations: E_{GAP}, energy gap; η, hardness; HOMO, highest occupied molecular orbital; LUMO, lowest unoccupied molecular orbital; S, softness; χ, electronegativity.
*Anti-obesity standard drug.

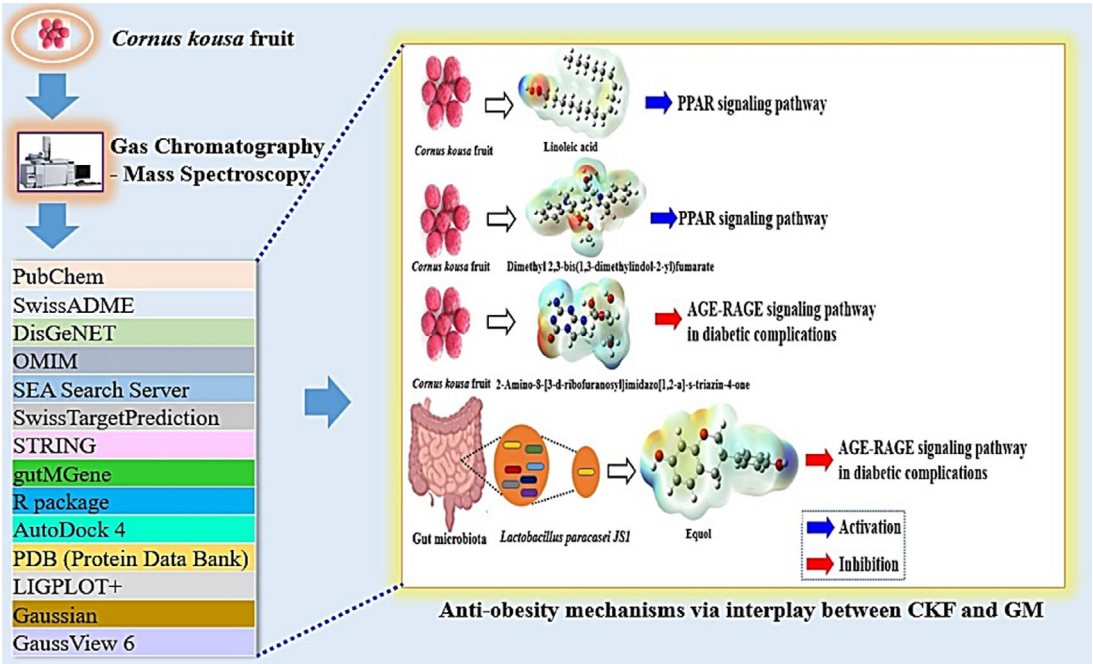


FIGURE 4 The key summary of this study.

might be a potent agent against OB. Our previous study clarified that equol converted by *L. paracasei JS1* can bind firmly to the active site on IL6 (Oh et al., 2022). Additionally, our result has shown that 2-amino-8-[3-D-ribofuranosyl]imidazo[1,2-a]-*s*-triazin-4-one from CKF exhibited good binding score on CDC42. Both CKF and GM were involved in the dampening of AGE-RAGE signaling pathway in diabetic complications.

The epidemiological evidence demonstrated that infants in the obese category during breastfeeding had a decreased pattern of *Enterococcus* compared with observed control groups (Laursen et al., 2020). It implies that *Enterococcus* is a significant microbe to modulate weight, which lines up with the CGSTM network analyses. *E. limosum* can covert natural polyphenols into favorable metabolites, which is a beneficial microbe to prevent OB in polyphenol–microbiota interconnections (Rios-Covian et al., 2019). *L. paracasei*, to be taken at 10^7–10^8 colony-forming unit/day for 10 weeks, exerts AOB effects in an obese mice model (Lee et al., 2021). As above-mentioned, CKF and GM are capable to alleviate OB via their orchestration in pharmacological space.

The intention of utilizing biological network module was to decrypt the intricated relationships between CKF and GM. NP is a powerful methodology to identify the relationships between targets and metabolites from CKF and GM. The application of the combined methodology has already been confirmed to diminish the error rate between the interpretation of a great amount of data in biological fields and its results (Gligorijević et al., 2016). Correspondingly, this study shows that the integrated pharmacological analysis with CKF and GM provides significant clues to uncover its nuanced relationships in the treatment on OB. In this context, more experimental data and its mechanistic studies are needed to obtain a better interpretation of the complicated matrix between CKF and GM.

5 | THE PROS AND CONS OF THIS STUDY

With the integrated pharmacological concept, we confirmed the therapeutic value of CKF and beneficial GM in the treatment of OB. The layout has been devised to decrypt interrelationships between CKF and GM, which is a platform mode to input new information. Moreover, with exactness and rigorousness, we introduced quantum chemistry theory to realize the drug-resemblance level of key compounds by comparison with a standard drug. In a way, this scenario shows that combinatorial study (bioinformatics, cheminformatics, pharmacology, microbiology, natural product chemistry, and quantum chemistry) can be beneficial to develop more significant effectors via extensive microbiome and nutrition against human disease. This setting might be a hallmark to advance further microbiome research as well as a new inflection point to unravel the unclarified relationships of exogenous species (herbal plant)–endogenous species (GM)–host (human).

In this report, the outputs obtained by the platform were significant elements to confirm the synergistic efficacy of CKF and GM against OB. From an entire viewpoint, the platform can be a significant toolkit to discover new findings on human diseases. The key summary of this study is unfolded in Figure 4.

6 | CONCLUSION

To summarize, PPARA-linoleic acid and FABP4-dimethyl 2,3-bis(1,3-dimethylindol-2-yl) fumarate from CKF act as agonists in PPAR signaling pathway, and IL6-equol from *L. paracasei JS1* and CDC42-2-amino-8-[3-D-ribofuranosyl] imidazo[1,2-a]-*S*-triazin-4-one from CKF act as an antagonist in the AGE-RAGE signaling pathway in diabetic complications function for relieving OB. This study showed that CKF and GM might have orchestrated effects against OB. Ultimately, the devised platform might be a standardized tool to unravel key mechanisms of diverse natural resources, prebiotics, probiotics, and postbiotics.

AUTHOR CONTRIBUTIONS

Ki-Kwang Oh contributed to study design, preparation, and drafting of the manuscript. Sang-Jun Yoon contributed to data collection and analysis. Sang Youn Lee, Satya Priya Sharma, Sung-Min Won, and Jin-Ju Jeong contributed to data curation. Dong Joon Kim was responsible for the supervision. Ki-Tae Suk contributed to the writing and revision of the manuscript.

ACKNOWLEDGMENTS

A preliminary version of this paper appeared as a Preprint (Oh et al., 2023) and was reelaborated during the authors' stay at Center for Microbiome, Institute for Liver and Digestive Diseases in February 2023 and May 2023, respectively. The authors wish to thank the Hallym university for exceptional working conditions. This study has been implemented with the support of the Hallym University Research Fund, the Basic Science Research Program through the National Research Foundation of Korea, funded by the Ministry of Education, Science and Technology.

Open access publishing is facilitated by Hallym University, the Basic Science Research Program through the National Research Foundation of Korea (NRF) is funded by the Ministry of Education, Science and Technology, Korea Institute for Advancement of Technology, and Bio Industrial Technology Development Program funded by the Ministry of Trade, Industry and Energy (MOTIE, Korea).

CONFLICT OF INTEREST STATEMENT

The authors declare that they have no conflicts of interest.

ORCID

Ki-Kwang Oh https://orcid.org/0000-0003-4199-7575

REFERENCES

Adole, V. A. (2021). Computational chemistry approach for the investigation of structural, electronic, chemical and quantum chemical facets of twelve Biginelli adducts. *Journal of Applied Organometallic Chemistry*, *1*(1), 29–40. https://doi.org/10.22034/JAOC.2021.278598.1009

Artham, S. M., Lavie, C. J., Milani, R. V., & Ventura, H. O. (2009). Obesity and hypertension, heart failure, and coronary heart disease—Risk factor, paradox, and recommendations for weight loss. *The Ochsner Journal*, *9*(3), 124.

Bresser, L. R. F., de Goffau, M. C., Levin, E., & Nieuwdorp, M. (2022). Gut microbiota in nutrition and health with a special focus on specific bacterial clusters. *Cells*, *11*(19), 3091. https://doi.org/10.3390/CELLS11193091

Chandrasekaran, C. V., Vijayalakshmi, M. A., Prakash, K., Bansal, V. S., Meenakshi, J., Amit, A., Chandrasekaran, C. V., Vijayalakshmi, M. A., Prakash, K., Bansal, V. S., Meenakshi, J., & Amit, A. (2012). Review article: Herbal approach for obesity management. *American Journal of Plant Sciences*, *3*(7), 1003–1014. https://doi.org/10.4236/AJPS.2012.327119

Cheng, L., Qi, C., Yang, H., Lu, M., Cai, Y., Fu, T., Ren, J., Jin, Q., & Zhang, X. (2022). gutMGene: A comprehensive database for target genes of gut microbes and microbial metabolites. *Nucleic Acids Research*, *50*(D1), D795–D800. https://doi.org/10.1093/NAR/GKAB786

Cheng, Z., Zhang, L., Yang, L., & Chu, H. (2022). The critical role of gut microbiota in obesity. *Frontiers in Endocrinology*, *13*, 1025706. https://doi.org/10.3389/FENDO.2022.1025706

Daina, A., Michielin, O., & Zoete, V. (2019). SwissTargetPrediction: Updated data and new features for efficient prediction of protein targets of small molecules. *Nucleic Acids Research*, *47*(W1), W357–W364. https://doi.org/10.1093/NAR/GKZ382

De Lile, J. R., Kang, S. G., Son, Y. A., & Lee, S. G. (2020). Do HOMO–LUMO energy levels and band gaps provide sufficient understanding of Dye-sensitizer activity trends for water purification? *ACS Omega*, *5*(25), 15052–15062. https://doi.org/10.1021/ACSOMEGA.0C00870/SUPPL_FILE/AO0C00870_SI_001.PDF

Ejtahed, H. S., Angoorani, P., Soroush, A. R., Hasani-Ranjbar, S., Siadat, S. D., & Larijani, B. (2020). Gut microbiota-derived metabolites in obesity: A systematic review. *Bioscience of Microbiota, Food and Health*, *39*(3), 65. https://doi.org/10.12938/BMFH.2019-026

Fan, Q., Xu, F., Liang, B., & Zou, X. (2021). The anti-obesity effect of traditional Chinese medicine on lipid metabolism. *Frontiers in Pharmacology*, *12*, 1486. https://doi.org/10.3389/FPHAR.2021.696603/BIBTEX

Gfeller, D., Michielin, O., & Zoete, V. (2013). Shaping the interaction landscape of bioactive molecules. *Bioinformatics*, *29*(23), 3073–3079. https://doi.org/10.1093/BIOINFORMATICS/BTT540

Gligorijević, V., Malod-Dognin, N., & Pržulj, N. (2016). Integrative methods for analyzing big data in precision medicine. *Proteomics*, *16*(5), 741–758. https://doi.org/10.1002/PMIC.201500396

Keiser, M. J., Roth, B. L., Armbruster, B. N., Ernsberger, P., Irwin, J. J., & Shoichet, B. K. (2007). Relating protein pharmacology by ligand chemistry. *Nature Biotechnology*, *25*(2), 197–206. https://doi.org/10.1038/NBT1284

Khan, M. I., Shin, J. H., Shin, T. S., Kim, M. Y., Cho, N. J., & Kim, J. D. (2018). Anthocyanins from *Cornus kousa* ethanolic extract attenuate obesity in association with anti-angiogenic activities in 3T3-L1 cells by down-regulating adipogeneses and lipogenesis. *PLoS ONE*, *13*(12), e0208556. https://doi.org/10.1371/JOURNAL.PONE.0208556

Laskowski, R. A., & Swindells, M. B. (2011). LigPlot+: Multiple ligand-protein interaction diagrams for drug discovery. *Journal of Chemical Information and Modeling*, *51*(10), 2778–2786. https://doi.org/10.1021/CI200227U/ASSET/IMAGES/LARGE/CI-2011-00227U_0005.JPEG

Laursen, M. F., Larsson, M. W., Lind, M. V., Larnkjær, A., Mølgaard, C., Michaelsen, K. F., Bahl, M. I., & Licht, T. R. (2020). Intestinal enterococcus abundance correlates inversely with excessive weight gain and increased plasma leptin in breastfed infants. *FEMS Microbiology Ecology*, *96*(5), 66. https://doi.org/10.1093/FEMSEC/FIAA066

Lee, S. Y., Shin, D. U., Kim, S. Y., Eom, J. E., Nam, Y. Do, Shin, H. S., Kim, J. E., & Woo, Y. H. (2021). Assessment the of anti-obesity effects and safety of *Lactobacillus paracasei* AO356. *Journal of the Korean Society of Food Science and Nutrition*, *50*(9), 904–911. https://doi.org/10.3746/JKFN.2021.50.9.904

Li, W., Yuan, G., Pan, Y., Wang, C., & Chen, H. (2017). Network pharmacology studies on the bioactive compounds and action mechanisms of natural products for the treatment of diabetes mellitus: A review. *Frontiers in Pharmacology*, *8*, 74. https://doi.org/10.3389/FPHAR.2017.00074/BIBTEX

Liu, Y., Sun, M., Yao, H., Liu, Y., & Gao, R. (2017). Herbal medicine for the treatment of obesity: An overview of scientific evidence from 2007 to 2017. *Evidence-Based Complementary and Alternative Medicine*, *2017*, 8943059. https://doi.org/10.1155/2017/8943059

Loging, W., Rodriguez-Esteban, R., Hill, J., Freeman, T., & Miglietta, J. (2011). Cheminformatic/bioinformatic analysis of large corporate databases: Application to drug repurposing. *Drug Discovery Today: Therapeutic Strategies*, *8*(3–4), 109–116. https://doi.org/10.1016/J.DDSTR.2011.06.004

Lucido, M. J., Orlando, B. J., Vecchio, A. J., & Malkowski, M. G. (2016). Crystal structure of aspirin-acetylated human cyclooxygenase-2: Insight into the formation of products with reversed stereochemistry. *Biochemistry*, *55*(8), 1226–1238. https://doi.org/10.1021/ACS.BIOCHEM.5B01378/ASSET/IMAGES/LARGE/BI-2015-013788_0005.JPEG

Matsson, P., & Kihlberg, J. (2017). How big is too big for cell permeability? *Journal of Medicinal Chemistry*, *60*(5), 1662–1664. https://doi.org/10.1021/ACS.JMEDCHEM.7B00237/ASSET/IMAGES/LARGE/JM-2017-00237V_0002.JPEG

Miar, M., Shiroudi, A., Pourshamsian, K., Oliaey, A. R., & Hatamjafari, F. (2021). Theoretical investigations on the HOMO–LUMO gap and global reactivity descriptor studies, natural bond orbital, and nucleus-independent chemical shifts analyses of 3-phenylbenzo[d]thiazole-2(3H)-imine and its para-substituted derivatives: Solvent and substituent effects. *Journal of Chemical Research*, *45*(1–2), 147–158. https://doi.org/10.1177/1747519820932091/ASSET/IMAGES/LARGE/10.1177_1747519820932091-FIG1.JPEG

Nuttall, F. Q. (2015). Body mass index: Obesity, BMI, and health: A critical review. *Nutrition Today*, *50*(3), 117–128. https://doi.org/10.1097/NT.0000000000000092

Oh, K.-K., Yoon, S.-J., Lee, S.-B., Lee, S. Y., Gupta, H., Ganesan, R., Sharma, S. P., Jeong, J.-J., Kim, D. J., & Suk, K.-T. (2023). The orchestration of Cornus kousa fruit and gut microbiota for anti- obesity via integrated pharmacological analysis based on metabolomics. Research Square. https://doi.org/10.21203/RS.3.RS-2842996/V1

Oh, K. K. (2022). Network pharmacology study to reveal underlying mechanisms, targets, and bioactives of *Aralia cordata* against obesity. *Network Modeling Analysis in Health Informatics and Bioinformatics*, *11*(1), 1–14. https://doi.org/10.1007/S13721-022-00372-4

Oh, K. K., Gupta, H., Min, B. H., Ganesan, R., Sharma, S. P., Won, S. M., Jeong, J. J., Lee, S. B., Cha, M. G., Kwon, G. H., Jeong, M. K., Hyun, J. Y., Eom, J. A., Park, H. J., Yoon, S. J., Choi, M. R., Kim, D. J., & Suk, K. T. (2022). Elucidation of prebiotics, probiotics, postbiotics, and target from gut microbiota to alleviate obesity via network pharmacology study. *Cells*, *11*(18), 2903. https://doi.org/10.3390/CELLS11182903

Pearson, R. G. (1986). Absolute electronegativity and hardness correlated with molecular orbital theory. *Proceedings of the National Academy of Sciences of the United States of America*, *83*(22), 8440. https://doi.org/10.1073/PNAS.83.22.8440

Poirier, H., Rouault, C., Clément, L., Niot, I., Monnot, M. C., Guerre-Millo, M., & Besnard, P. (2005). Hyperinsulinaemia triggered by dietary conjugated linoleic acid is associated with a decrease in leptin and adiponectin plasma levels and pancreatic beta cell hyperplasia in the mouse. *Diabetologia*, *48*(6), 1059–1065. https://doi.org/10.1007/S00125-005-1765-8

Preuss, H. G., Bagchi, M., Bagchi, D., & Kaats, G. R. (2010). Obesity and cancer. *The Oncologist*, *15*(6), 197–204. https://doi.org/10.1634/THEONCOLOGIST.2009-0285

Rayalam, S., Della-Fera, M. A., & Baile, C. A. (2008). Phytochemicals and regulation of the adipocyte life cycle. *The Journal of Nutritional Biochemistry*, *19*(11), 717–726. https://doi.org/10.1016/J.JNUTBIO.2007.12.007

Rios-Covian, D., Nagpal, R., Angelina, T., Corrêa, F., Rogero, M. M., Mariko, N., Hassimotto, A., & Lajolo, F. M. (2019). The two-way polyphenols-microbiota interactions and their effects on obesity and related metabolic diseases. *Frontiers in Nutrition*, *6*, 188. https://doi.org/10.3389/FNUT.2019.00188

Schneider, G. F., Salazar, D., Hildreth, S. B., Helm, R. F., & Whitehead, S. R. (2021). Comparative metabolomics of fruits and leaves in a hyperdiverse lineage suggests fruits are a key incubator of phytochemical diversification. *Frontiers in Plant Science*, *12*, 1802. https://doi.org/10.3389/FPLS.2021.693739/BIBTEX

Shahinozzaman, M., Taira, N., Ishii, T., Halim, M. A., Hossain, M. A., & Tawata, S. (2018). Anti-inflammatory, anti-diabetic, and anti-Alzheimer's effects of prenylated flavonoids from Okinawa propolis: An investigation by experimental and computational studies. *Molecules (Basel, Switzerland)*, *23*(10), 2479. https://doi.org/10.3390/MOLECULES23102479

Shityakov, S., & Förster, C. (2014). In silico predictive model to determine vector-mediated transport properties for the blood-brain barrier choline transporter. *Advances and Applications in Bioinformatics and Chemistry : AABC*, *7*(1), 23–36. https://doi.org/10.2147/AABC.S63749

Silvarajoo, S., Osman, U. M., Kamarudin, K. H., Razali, M. H., Yusoff, H. M., Bhat, I. U. H., Rozaini, M. Z. H., & Juahir, Y. (2020). Dataset of theoretical molecular electrostatic potential (MEP), highest occupied molecular orbital-lowest unoccupied molecular orbital (HOMO–LUMO) band gap and experimental cole-cole plot of 4-(ortho-, meta- and para-fluorophenyl)thiosemicarbazide isomers. *Data in Brief*, *32*, 106299. https://doi.org/10.1016/J.DIB.2020.106299

Singh, N., Chaput, L., & Villoutreix, B. O. (2021). Virtual screening web servers: Designing chemical probes and drug candidates in the cyberspace. *Briefings in Bioinformatics*, *22*(2), 1790–1818. https://doi.org/10.1093/BIB/BBAA034

Soo, H. C., Chung, F. F. L., Lim, K. H., Yap, V. A., Bradshaw, T. D., Hii, L. W., Tan, S. H., See, S. J., Tan, Y. F., Leong, C. O., & Mai, C. W. (2017). Cudraflavone C induces tumor-specific apoptosis in colorectal cancer cells through inhibition of the phosphoinositide 3-kinase (PI3K)-AKT pathway. *PLoS ONE*, *12*(1), e0170551. https://doi.org/10.1371/JOURNAL.PONE.0170551

Szklarczyk, D., Gable, A. L., Nastou, K. C., Lyon, D., Kirsch, R., Pyysalo, S., Doncheva, N. T., Legeay, M., Fang, T., Bork, P., Jensen, L. J., & von Mering, C. (2021). The STRING database in 2021: Customizable protein-

protein networks, and functional characterization of user-uploaded gene/measurement sets. *Nucleic Acids Research*, *49*(D1), D605–D612. https://doi.org/10.1093/NAR/GKAA1074

Szumilak, M., Wiktorowska-Owczarek, A., & Stanczak, A. (2021). Hybrid drugs—A strategy for overcoming anticancer drug resistance? *Molecules*, *26*(9), 2601. https://doi.org/10.3390/MOLECULES26092601

Tak, Y. J., & Lee, S. Y. (2021). Anti-obesity drugs: Long-term efficacy and safety: An updated review. *The World Journal of Men's Health*, *39*(2), 208–221. https://doi.org/10.5534/WJMH.200010

Tantardini, C., & Oganov, A. R. (2021). Thermochemical electronegativities of the elements. *Nature Communications*, *12*(1), 1–9. https://doi.org/10.1038/s41467-021-22429-0

Tremmel, M., Gerdtham, U. G., Nilsson, P. M., & Saha, S. (2017). Economic burden of obesity: A systematic literature review. *International Journal of Environmental Research and Public Health*, *14*(4), 435. https://doi.org/10.3390/IJERPH14040435

Vetrivel, P., Murugesan, R., Bhosale, P. B., Ha, S. E., Kim, H. H., Heo, J. D., & Kim, G. S. (2021). A network pharmacological approach to reveal the pharmacological targets and its associated biological mechanisms of prunetin-5-*O*-glucoside against gastric cancer. *Cancers*, *13*(8), 1918. https://doi.org/10.3390/CANCERS13081918/S1

Wendel, A. A., Purushotham, A., Liu, L. F., & Belury, M. A. (2008). Conjugated linoleic acid fails to worsen insulin resistance but induces hepatic steatosis in the presence of leptin in ob/ob mice. *Journal of Lipid Research*, *49*(1), 98–106. https://doi.org/10.1194/JLR.M700195-JLR200

Zhang, Y. J., Sun, Y. Z., Gao, X. H., & Qi, R. Q. (2019). Integrated bioinformatic analysis of differentially expressed genes and signaling pathways in plaque psoriasis. *Molecular Medicine Reports*, *20*(1), 225. https://doi.org/10.3892/MMR.2019.10241

Zheng, C., Chen, X. K., Tian, X. Y., Ma, A. C. H., & Wong, S. H. S. (2022). Does the gut microbiota contribute to the antiobesity effect of exercise? A systematic review and meta-analysis. *Obesity*, *30*(2), 407–423. https://doi.org/10.1002/OBY.23345

Zheng, D., Liwinski, T., & Elinav, E. (2020). Interaction between microbiota and immunity in health and disease. *Cell Research*, *30*(6), 492–506. https://doi.org/10.1038/s41422-020-0332-7

SUPPORTING INFORMATION

Additional supporting information can be found online in the Supporting Information section at the end of this article.

How to cite this article: Oh, K. K, Yoon, S. J., Lee, S. Y., Sharma, S. P., Won, S. M., Jeong, J. J., Kim, D. J., & Suk, K. T. (2024). The orchestrated feature of *Cornus kousa* fruit and gut microbiota against obesity via integrated pharmacology. *Food Frontiers*, *5*, 2262–2274. https://doi.org/10.1002/fft2.435